IEEE Access
Multidisciplinary | Rapid Review | Open Access Journal

Received January 26, 2019, accepted February 17, 2019, date of publication February 21, 2019, date of current version March 20, 2019.

Digital Object Identifier 10.1109/ACCESS.2019.2900503

A Novel Fault Diagnosis Method of Gearbox Based on Maximum Kurtosis Spectral Entropy Deconvolution

ZHIJIAN WANG, JIE ZHOU, JUNYUAN WANG, WENHUA DU, JINGTAI WANG, XIAOFENG HAN, AND GAOFENG HE

College of Mechanical Engineering, North University of China, Taiyuan 030051, China

Corresponding author: Junyuan Wang (wangyi01161013@163.com)

This work was supported in part by the Shanxi Provincial Natural Science Foundation of China under Grant 201801D121186, Grant 201801D221237, and Grant 201601D102035, and in part by the Science Foundation of the North University of China under Grant XJJ201802.

ABSTRACT Minimum entropy deconvolution (MED) is widely used in the gearbox fault diagnosis because it can enhance the energy of the impact signal. However, it is sensitive to single abnormal impulsive oscillation. This is because it takes kurtosis as the objective function and solves the optimal filter by iteration. In addition, the filter length is not adaptive and needs to be determined artificially. This paper proposes a maximum kurtosis spectral entropy deconvolution (MKSED) method and applies it to bearing fault diagnosis. Considering that the kurtosis spectral entropy has the advantage of highlighting the continuous impact oscillation, the kurtosis spectral entropy is chosen as the objective function of deconvolution. At the same time, kurtosis spectral entropy is also used as the fitness function of improved local particle swarm optimization algorithm (LPSO), and the filter length is optimized by LPSO, which makes that MKSED adaptively determines the length of the filter while solving the deconvolution, so that it can accurately extract the continuous pulse signal. The results of the simulation signal analysis show that the proposed MKSED method is superior to MED, and the proposed method is applied to bearing fault diagnosis, which verifies its ability to extract continuous impact.

INDEX TERMS Minimum entropy deconvolution, particle swarm optimization, maximum kurtosis spectral entropy deconvolution, fault diagnosis.

I. INTRODUCTION

As the most commonly used rotating machinery, rolling bearing faults are very common, including outer ring, inner ring and rolling element faults [1]. These faults are characterized by the periodic impact. However, when the fault occurs, due to the complex environment, the vibration signal collected by the sensor often has a lot of background noise. These impulsive signals are often submerged by noise, so it is very important to quickly and accurately find the location of bearing fault. In other words, reasonable and effective noise reduction methods are very important for the development of fault diagnosis. So far, there are many common methods for fault diagnosis of rotating machinery, including autoregressive models [3], spectral kurtosis [4], cyclostationary theory [5], Empirical Mode Decomposition (EMD) [6], Ensemble Empirical Mode Decomposition (EEMD) [7], Variational Mode Decomposition (VMD) [8] and so on.

Since 2012, this is easy to find that MED has been widely used in fault diagnosis of rotating machinery because it can detect impulse components in fault signals. The purpose of MED is to extract fault components from impulse signals by maximizing kurtosis and to further solve filter [10]. In recent years, EEMD has been widely used in fault diagnosis and fault feature extraction in strong noise environment [11], [12]. The purpose of EEMD is to overcome the mode aliasing of EMD by noise-assisted analysis method [13]. However, considering that the noise cannot be completely neutralized, which makes the EEMD still exist modal aliasing phenomenon, Wang *et al.* [14] proposed a combination of MED and EEMD, which avoided

The associate editor coordinating the review of this manuscript and approving it for publication was Jun Shi.

successfully the modal aliasing phenomenon of EEMD and applied it to the fault diagnosis of the gearbox. At the same time, Wang *et al.* [15] proposed a method combining local mean decomposition (LMD) with MED to overcome the modal aliasing of LMD. Endo and Randall [16] combined MED technology with the autoregressive model, proposed a new deconvolution technology and applied it to fault signal extraction of the gearbox, which proved its feasibility. Sawalhi *et al.* [17] presented an algorithm for enhancing the surveillance capability of spectral kurtosis (SK) by using the minimum entropy deconvolution (MED) technique, and verified its effectiveness through bearing failure experiments. Considering that MED can only extract a single impulse, to improve the shortcomings of MED, McDonald *et al.* [18] proposed a new method called maximum correlation kurtosis deconvolution (MCKD) and validated its effectiveness by simulation signals. With its good deconvolution performance, MCKD can extract multiple impulse signals [9], [19]. However, although MCKD is more effective than MED, the noise reduction accuracy of MCKD is limited by multiple parameters and resampling process. In order to solve these shortcomings, Miao *et al.* [9] proposed an improved maximum correlation kurtosis deconvolution (IMCKD) method to update the fault cycle iteratively according to the autocorrelation function of the envelope signal to prevent the resampling process. IMCKD validates the effectiveness of the method through simulation and experimental analysis.

In MED technology and its extended version, the selected iteration objective function is kurtosis maximization [20]. At the initial stage of rotating machinery failure, the kurtosis index increases obviously, but with the emergence of many periodic pulses, the kurtosis value decreases. Therefore, the kurtosis index is very sensitive to the transient pulse. The kurtosis value of a single impulse is larger. When a series of impulse signals appear, the kurtosis value will become smaller. However, the best result we need is to denoise and highlight more impulsive pulses through MED. So, if we want to get the best result, we need to improve MED from the source. In other words, we need to find a parameter that can reflect more periodic pulses to replace the objective function of MED to achieve the purpose of improving MED.

In this paper, a new index, Kurtosis Spectral Entropy (KSE), is proposed. The parameter consists of two parts, one is Kurtosis value, the other is Envelope Spectrum Entropy. When there are multiple periodic pulses in rotating machinery, the main components of envelope spectrum are concentrated in the low frequency range after envelope spectrum analysis of periodic signals, which leads to the reduction of envelope spectrum entropy. Therefore, the envelope spectral entropy can express the uniformity of periodic pulses. The more pulses detected, the clearer the envelope spectrum and the smaller the envelope spectrum entropy [23]. In fact, the kurtosis spectral entropy proposed in this paper is the ratio of kurtosis to envelope spectral entropy. This definition not only keeps the original characteristics of MED, but also increases the uniformity of periodic pulses. At the same time, the effective diagnosis of complex faults is considered. This paper first denoises the original signal by EEMD, then removes the high-frequency noise and the intrinsic mode function with less correlation, and resolves the mode mixing of EEMD by reconstructing the mode function. EEMD can decompose the components of different frequencies into different time scales, and then use MKSED to enhance the impact of different periods to obtain good diagnostic results. Finally, the effective intrinsic mode function is determined as the object of deconvolution, and the kurtosis spectral entropy is used as the objective function to solve the inverse filter. At the same time, the kurtosis spectral entropy is used as the fitness function of particle swarm optimization, and the filter length is optimized by improved particle swarm optimization. By calculating the kurtosis spectral entropy of each layer intrinsic mode function and taking its maximum as the objective function, the noise reduction effect of MED is further improved. This method is called MKSED.

This paper verifies that MKSED has better noise reduction effect than MED and MCKD through simulation and measurement signals, and applies it to gear box fault diagnosis.

II. THEORETICAL FOUNDATIO

A. MINIMUM ENTROPY DECONVOLUTION

Minimum Entropy Deconvolution (MED) was first proposed by Wiggins [22], which is a filtering method to maximize the kurtosis of the original signal. In 2007, Sawalhi *et al.* [17] applied the MED method to the diagnosis of rolling bearings and gears. The purpose of the MED algorithm is to increase the signal-to-noise ratio of the signal with the maximum value of the kurtosis as the iterative termination condition. Therefore, it is widely used in fault diagnoses such as gears and bearings.

MED is to eliminate the influence of transmission path by the optimized filter. $x_n\,(n = 1, 2, \cdots, N)$ is the input vibration signal sequence, which includes random noise, periodic impact, harmonics and so on. The output signal generated by the input signal x_n and the FIR filter $f = [f_1, f_2, \cdots, f_L]$ can be expressed as follows:

$$y_n = \sum_{l=1}^{L} f_l x_{n-l} \tag{1}$$

The output y_n should coincide with the impulse signal of the original signal as far as possible. If a shock signal corresponds to a larger kurtosis value, then the filter of MED must maximize the kurtosis of the output signal. The kurtosis of the zero means of the output signal y_n is defined as follows:

$$k\,(f) = \frac{\sum_{n=1}^{N} y_n^4}{\left(\sum_{n=1}^{N} y_n^2\right)^2} \tag{2}$$

The optimal solution f_{optimal} maximizes the kurtosis of the output signal, $K\left(f_{\text{optimal}}\right) \geq K\,(f)\,, \forall f \in R^L$, R^L is an L-dimensional Euclidean space, K represents the kurtosis in formula (2) and f represents a filter of arbitrary length L.

The iteration formula of the iteration process is as follow:

$$f = \frac{\sum_{n=1}^{N} y_n^2}{\sum_{n=1}^{N} y_n^4} \left(X_0 X_0^T\right)^{-1} X_0 \left[y_1^3\ y_2^3\ \cdots\ y_N^3\right] \tag{3}$$

where

$$X_0 = \begin{bmatrix} x_1 & x_2 & x_3 & & x_N \\ 0 & x_1 & x_2 & \cdots & x_{N-1} \\ 0 & & x_1 & & x_{N-2} \\ & \vdots & & \ddots & \vdots \\ 0 & 0 & 0 & \cdots & x_{N-L+1} \end{bmatrix}_{L\times N}$$

Details of this algorithm, including the deduction of the iteration formula and the stopping criteria of the iteration algorithm, can be found in [22].

We can note that the MED solves the inverse filter based on kurtosis maximization rather than minimizing entropy. Although there is a certain relationship between kurtosis and entropy, its basis is still to maximize kurtosis. Thus, MED finds the source with maximum kurtosis rather than minimum entropy. This is the most important reason for the unimodality of MED results.

B. IMPROVED PARTICLE SWARM OPTIMIZATION

Particle swarm optimization (PSO) algorithm has good global optimization ability. Suppose there are M particles in D-dimensional space, which constitute particle space $X = (X_1, X_2, \cdots, X_M)$. Each particle is a D-dimensional vector, and the vector of the t-th particle is $X_i = (X_{i1}, X_{i2}, \cdots, X_{iD})$, which represents the position of the t-th particle in the D-dimensional search space. The velocity of the t-th particle is $V_i = (V_{i1}, V_{i2}, \cdots, V_{in})$, the individual historical optimal solution $P_i = (P_{i1}, P_{i2}, \cdots, P_{in})$, and the global optimal solution $G = (g_1, g_2, \cdots, g_n)$ in the whole space. As the iteration progresses, the velocity and position of the particle are updated as follows:

$$\begin{aligned} v_{id}^{k+1} &= \omega \times v_{id}^{k} + c1 \times rand \times (P_i - x_{id}^{k}) \\ &\quad + c2 \times rand \times (\mathrm{G} - x_{id}^{k}) \end{aligned} \tag{4}$$

$$x_{id}^{k+1} = x_{id}^{k} + v_{id}^{k+1} \tag{5}$$

where: ω is the inertia factor; i =1,2,..,M; d =1,2, ..., D; k is the current iteration number; c1,c2 is the learning factor of particles; Rand is the random number between [0,1].

The above is the standard PSO algorithm. However, it has the disadvantage of easily falling into a local optimum. Therefore, this paper optimizes the parameters of MKSED through the improved local PSO algorithm (LPSO). By improving the speed update formula of PSO, the global historical optimal solution g of the particle swarm is replaced by the optimal solution P_{next} of the particles in the neighborhood of the particle, so that the particle swarm velocity update is no longer dependent on the global optimal, and it is not easy to fall into the local optimal solution. The improved speed update formula is:

$$\begin{aligned} v_{id}^{k+1} &= \omega \times v_{id}^{k} + c1 \times rand \times (P_i - x_{id}^{k}) \\ &\quad + c2 \times rand \times (P_{inext} - x_{id}^{k}) \end{aligned} \tag{6}$$

where, P_{inext} is the optimal solution of the particles in the neighborhood of the i-th particle.

From [8], it is found that in order to obtain better convergence effect for the velocity change in particle swarm optimization algorithm and obtain more accurate results, the inertia factor changes according to concave function is better than linear change, and linear change is better than constant change. Therefore, the concave function is used in this paper to change with the number of iterations.

$$\begin{aligned} \omega &= (\omega_{\max} - \omega_{\min}) \times \left(\frac{k}{\max gen}\right)^2 \\ &\quad + (\omega_{\max} - \omega_{\min}) \times \left(2 \times \frac{k}{\max gen}\right) + \omega_{\max} \end{aligned} \tag{7}$$

where, $\omega_{\max}$ is the maximum of ω; $\omega_{\min}$ is the minimum of ω; k is the number of iterations of particle swarm optimization; max gen is the total number of iterations of PSO algorithm.

In the standard particle swarm algorithm, the learning factors cl, c2 are generally constant values. But according to the experiment, the learning factor which changes with iteration can get better convergence effect. That is, in the early stage of particle evolution, the particles can search carefully in their own neighborhood to prevent the particles from convergence to the local optimal solution [23]. At the later stage of evolution, PSO should converge to the global optimal solution faster and more accurately. That is to say, in the initial stage, the value of c1 will be larger, while in the later stage, the value of c2 will increase with the number of iterations. So, the improved learning factor formula is:

$$c_1 = 4 - e^{-\left|\frac{1}{M}\sum_{i=1}^{M}(P_i - G)\right|} \tag{8}$$

$$c_2 = 4 - c_1 \tag{9}$$

When searching for the optimal solution, particle swarm optimization needs to choose a fitness function to measure the effect of the optimal solution. When the particle updates a position, it needs to calculate the fitness value of each time according to the fitness function, and select the optimal solution by comparison. The traditional fitness function chooses signal-to-noise ratio, kurtosis and entropy as the fitness function to evaluate the noise reduction effect of MED. The main idea of this paper is to reflect the continuous impulsive signal of the original vibration signal through the results of MED noise reduction, so the kurtosis is not suitable. In order to highlight the pulse of the continuous periodic signal, the kurtosis spectral entropy is selected as the filter effect of MED. The specific concept of kurtosis spectral entropy is shown in the following section.

C. MAXIMUM KURTOSIS SPECTRUM ENTROPY DECONVOLUTION METHOD

Kurtosis index is sensitive to transient impulse signals and is widely used in gear box fault diagnosis. However, the kurtosis is only sensitive to a single impulse, and when multiple impulses exist simultaneously, the kurtosis decreases. When

an early failure occurs in gear or bearing, the kurtosis index increases significantly. However, kurtosis is not suitable for describing impact vibrations with periodicity. On the contrary, the envelope spectrum entropy can express the uniformity of periodic pulses. When the number of pulses is detected, the envelope spectrum is clear and the envelope spectral entropy is smaller.

Assuming that $S_R(\omega)$ represents the envelope spectrum of the original signal and j is the number of components decomposed by EEMD, the envelope spectrum can be evenly divided into j frequency intervals along the frequency axis, and the percentage of the i-th interval can be described as B, which satisfies:

$$\sum_{i=1}^{J} P_i\left(S_R(\omega)\right) = 1 \tag{10}$$

Therefore, the envelope spectral entropy is defined

$$Es = -\sum_{i=1}^{J} P_i\left(S_R(i)\right) \ln P_i\left(S_R(i)\right) \tag{11}$$

where, $P_i\left(S_R(i)\right) = S_R(i) \Big/ \sum_{j=1}^{N} S_R(j)$.

Kurtosis represents the impact characteristics of signals, envelope spectral entropy represents the periodic characteristics of signals, and a new index kurtosis spectral entropy can be expressed as follows:

$$KSE(x) = \frac{kurt(x)}{Es} \tag{12}$$

where, $kurt(x)$ represents the kurtosis of the input signal and $KSE(x)$ represents the kurtosis spectral entropy of the signal. Obviously, for the periodic impulse signal, the envelope spectrum is concentrated in the low frequency region, resulting in a smaller value of Es. Sporadic impulse signals lead to larger envelope spectral entropy, so $KSE(x)$ can reflect the uniformity of periodic impulse signals. The same intrinsic mode function obtained by EEMD decomposition is reconstructed, and MKSED is used to denoise the EEMD and extract more uniform periodic pulses.

$$KSE(x) = \frac{kurt(IMF_i)}{Es} \tag{13}$$

In actual working conditions, noise often affects the extraction of fault features. Selecting appropriate indicators for deconvolution and adaptive selection of filter length are the key to extract and analyze bearing fault features using MKSED. Using KSE as the objective function of deconvolution can highlight most of the impact signals. Here, the IMF is assumed to be time series $x(n)$, then:

$$KSE\left(f(l)\right) = \frac{-\sum_{n=1}^{N} x^4(n)}{\left(\sum_{n=1}^{N} x^2(n)\right)^2 \left(\sum_{i=1}^{N} p_i \cdot \ln p_i\right)} \tag{14}$$

Then, by combination with equation (11) and taking the derivatives of equation (14) with respect to filter coefficients f, and solving it equal to zero:

$$\frac{\partial KSE\left(f(n)\right)}{\partial f(l)} = 0 \tag{15}$$

The following equation can be obtained from the deconvolution process:

$$\frac{\partial x(n)}{\partial f(l)} = m(n-l) \tag{16}$$

where, $m(n)$ Is a sequence of outputs. Formula 16 is introduced into 15 to obtain:

$$\underbrace{\frac{4\sum_{n=1}^{N} x^3(n)\left(\sum_{i=1}^{N} P_i(S_R(i)) \cdot \ln P_i\left(S_R(i)\right)\right) \cdot m(n-l)}{4\sum_{n=1}^{N} x^2(n) + \left(\sum_{n=1}^{N} x^2(n)\right)^2 \left(\sum_{i=1}^{N} \left(1 + \ln P_i\left(S_R(i)\right)\right)\right)}}_{b} = \underbrace{\sum_{n=1}^{N} m(n-l)\, m(n-p)}_{A} \cdot \underbrace{\sum_{p=1}^{L} f(p)}_{f} \tag{17}$$

Eq. (17) can be written in matrix form:

$$b = A \times f \tag{18}$$

The inverse filter matrix can be calculated iteratively by Eq. (18):

$$f = A^{-1} \times b \tag{19}$$

However, when multiple faults coexist, different fault features need to be decomposed into different intrinsic mode function. Therefore, the signal needs to be decomposed by EEMD. It can not only eliminate the high noise component unrelated to the original signal, but also decompose different time scales into different intrinsic mode function. Considering the existence of mode mixing in EEMD, the idea of reconstructing modal function is introduced to improve the energy of the impact signal while eliminating mode mixing. In order to determine the filter length adaptively, LPSO is used to optimize the filter length, which not only avoids the subjectivity of artificial setting, but also improves the accuracy of parameter selection. Finally, the envelope spectrum analysis of the denoised signal is carried out to determine the final fault characteristics.

1) Firstly, the vibration signals are decomposed by EEMD.
2) Determine whether there is modal mixing, and remove the high frequency noise component and the eigenmode function with weak correlation.
3) If there is modal mixing, the same mode function is reconstructed to obtain CMF1, CMF2, etc.
4) Solve the envelope spectrum of the above eigenmode function and calculate the kurtosis and Es.
5) Calculate the kurtosis spectral entropy KSE.
6) Set the particle population size M and the number of iterations N in the LPSO algorithm, set the maximum and minimum values of the inertia factor, and initialize L. In order to cover the whole frequency band

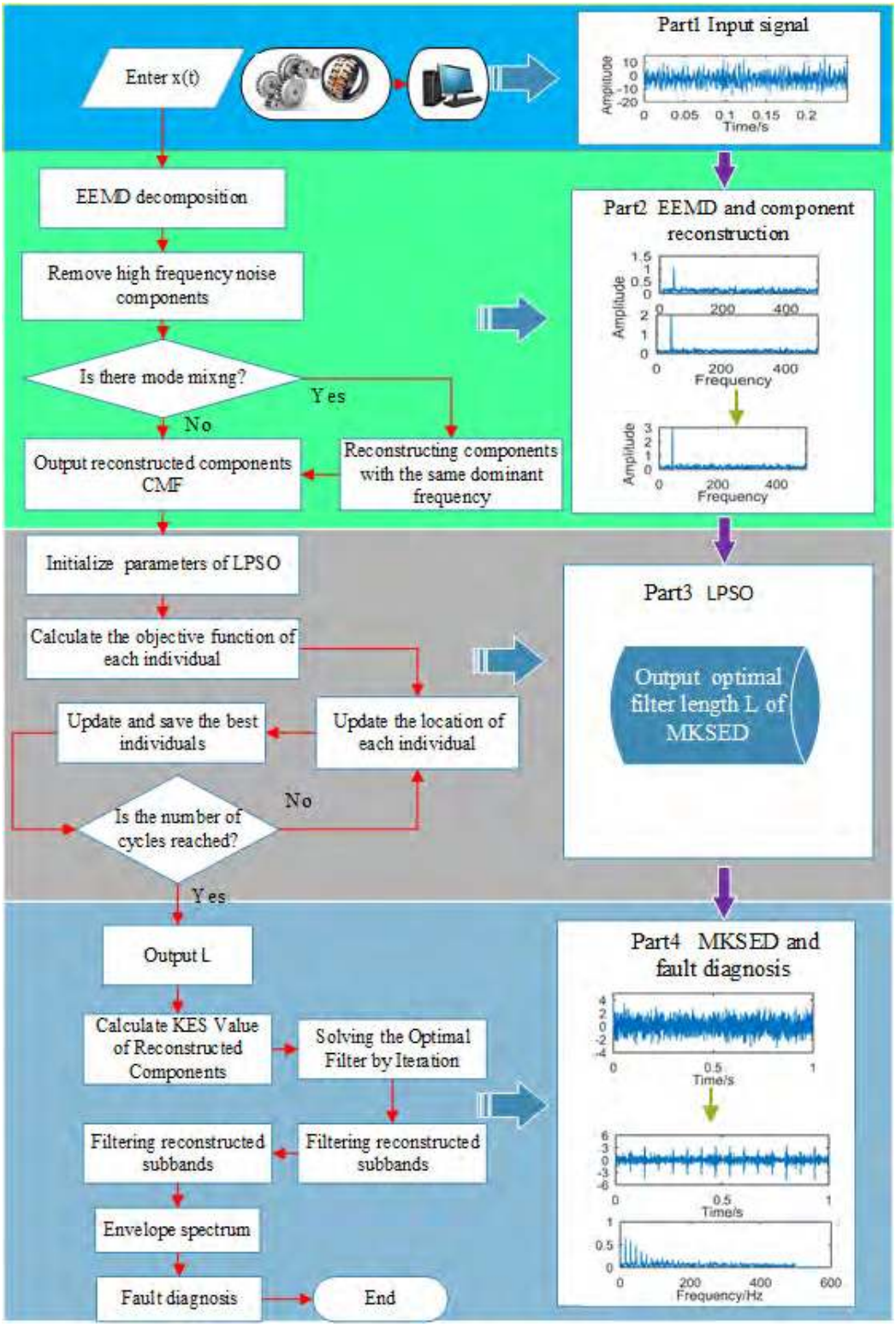

FIGURE 1. Flow chart of the proposed method.

of the fault accurately, L should satisfy the inequality $L > 2\mathrm{Fm} / \mathrm{Fs}$, where Fm is the fault characteristic frequency and Fs is the sampling frequency.

7) The L and signal are input into the improved LPSO. The improved LPSO is used to optimize the filter length of MKSED, and the optimal solution L_0 is obtained.

8) The obtained optimal length L0 is input to the MKSED filter, and the kurtosis spectral entropy of the fifth step is used as an objective function to denoise the MKSED for CMF1 and CMF2. The optimal filter is obtained and the denoised signal is output.
9) The output is demodulated by the envelope spectrum to determine the fault characteristic.

The algorithm flow of the proposed method is shown in Figure 1.

III. SIMULATION

When the gear is spalled and the inner and outer rings of the bearing are cracked, the vibration signal is expressed as periodic pulses and noise. In this paper, a periodic vibration signal is given as shown in equation (20), in which the natural frequency is 300 Hz and the periodic shock frequency is 50 Hz. The sampling points are 2000.

$$x_3(t) = A_m \times \exp(-\frac{g}{T_m}) \sin(2\pi f_c t) + 0.5 \times randn(t)$$
$$A_m = 1.1, g = 0.1, T_m = 1/50, f_c = 300Hz \quad (20)$$

Figure 2 shows the time-domain graph and the envelope spectrum of the simulated signal. It can be observed that the impact is submerged by noise. There is no obvious periodic pulse in the time domain graph, and the envelope spectrum is also disorderly, which contains a lot of noise.

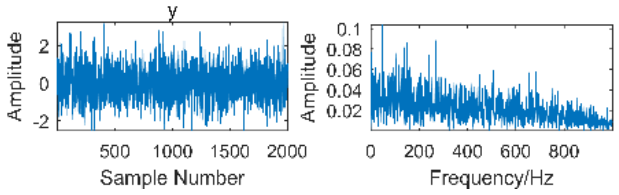

FIGURE 2. Time domain waveform and envelope analysis of simulation signals.

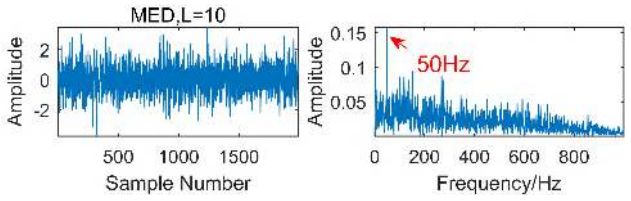

FIGURE 3. Time domain waveform and envelope spectrum of the simulated signal after noise reduction by MED at L=10.

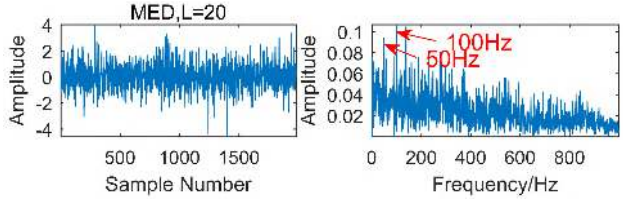

FIGURE 4. Time domain waveform and envelope spectrum of the simulated signal after noise reduction by MED at L=20.

Figure.3-8 shows the results obtained by MED with different filter lengths. The corresponding filter lengths L are

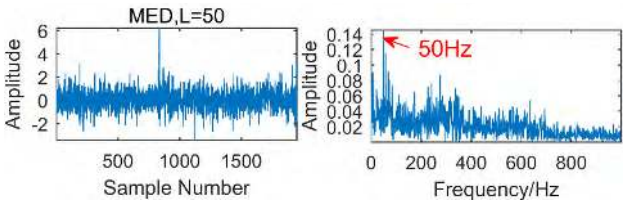

FIGURE 5. Time domain waveform and envelope spectrum of the simulated signal after noise reduction by MED at L=30.

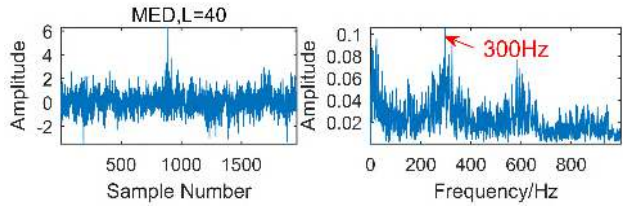

FIGURE 6. Time domain waveform and envelope spectrum of the simulated signal after noise reduction by MED at L=40.

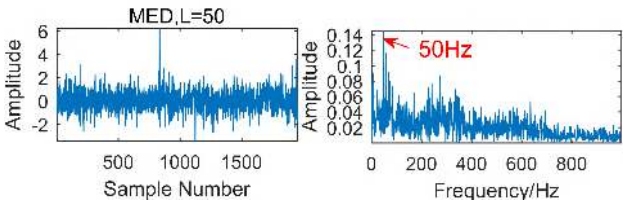

FIGURE 7. Time domain waveform and envelope spectrum of the simulated signal after noise reduction by MED at L=50.

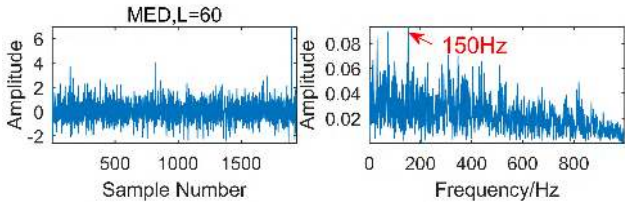

FIGURE 8. Time domain waveform and envelope spectrum of the simulated signal after noise reduction by MED at L=60.

10, 20, 30, 40, 50, and 60, respectively. Figure.3 shows the results of MED at L = 10. It can be seen that the peak value of time domain waveform increases little and the noise component decreases somewhat. In the envelope spectrum, there is an obvious peak at 50Hz, which corresponds to the fault cycle. Figure.4 shows the results of MED at L = 20. The peak value of time domain waveform increases obviously, and there are obvious peaks at 50Hz and 100Hz in the envelope spectrum, which corresponds to the fault frequency and its twice. With the increase of L, it can be observed that the peak value of time domain waveform increases, but the number of enhanced pulses decreases. As shown in Figure.6 and Figure.7, There are obvious single pulses in the time domain graph, which is due to the principle of MED. Therefore, MED does not extract pulses well, and there are limitations in the diagnosis of rotating machinery faults.

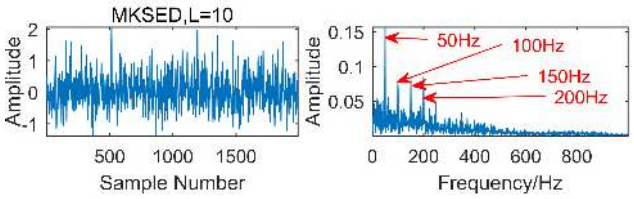

FIGURE 9. Time domain waveform and envelope spectrum of the simulated signal after noise reduction by MKSED at L=10.

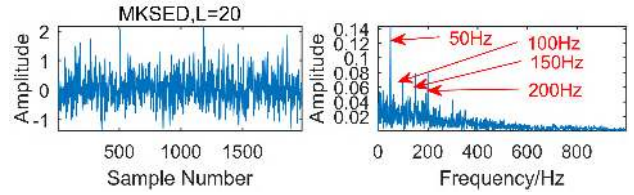

FIGURE 10. Time domain waveform and envelope spectrum of the simulated signal after noise reduction by MKSED at L=20.

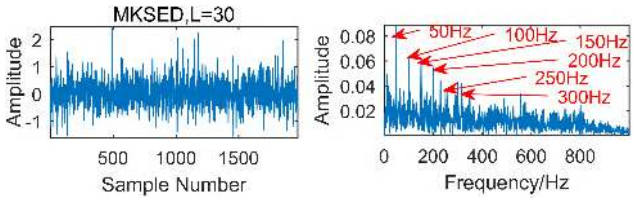

FIGURE 11. Time domain waveform and envelope spectrum of the simulated signal after noise reduction by MKSED at L=30.

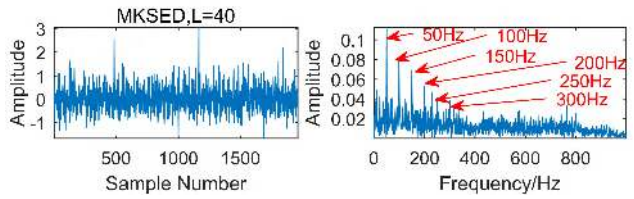

FIGURE 12. Time domain waveform and envelope spectrum of the simulated signal after noise reduction by MKSED at L=40.

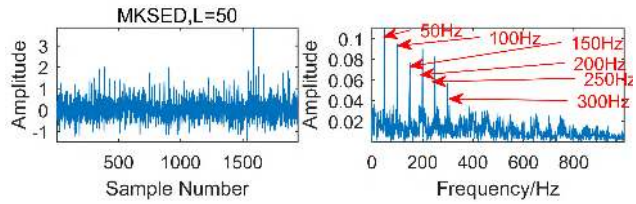

FIGURE 13. Time domain waveform and envelope spectrum of the simulated signal after noise reduction by MKSED at L=50.

Figure.9-14 shows the results obtained by MKSED with different filter lengths. The corresponding filter lengths L are 10, 20, 30, 40, 50, and 60, respectively. Figure.9 shows the results of MKSED at L = 10. It can be seen that the peak value of time domain waveform increases and the noise component decreases somewhat. In the envelope spectrum, there are obvious peaks at 50Hz, 100Hz, 150Hz and 200Hz, which correspond to the fault frequency and its double, triple and quadruple respectively. Compared with the results of

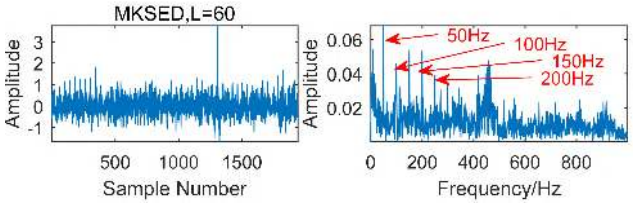

FIGURE 14. Time domain waveform and envelope spectrum of the simulated signal after noise reduction by MKSED at L=60.

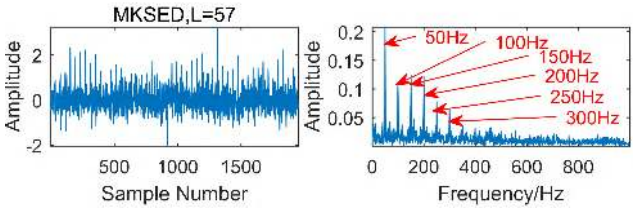

FIGURE 15. Time domain waveform and envelope spectrum of the simulated signal after noise reduction by MKSED at L=57.

MED at L=10 shown in Figure.3, the effect of MKSED is significantly better than that of MED. With the increase of L, the peak value of time domain waveform will increase, and the fault frequency and its multiple shown in envelope spectrum will become clearer and clearer. Figure.11 shows the results of MKSED at L = 30. In the envelope spectrum, the peak value appears at the fault frequency and at its double, triple, quadruple, quintuple and six times. However, as the filter length continues to increase, the effect of MKSED will also decline. Figure. 13 shows the processing result of MKSED at L = 60. It can be observed that the pulse uniformity of the time domain waveform is degraded, and the fault period of the envelope spectrum extraction is also disordered. It is easy to understand that the filter length also has a great influence on the results of MKSED, which needs to be optimized.

Figure. 15 shows the results of signal processing by optimized MKSED. The filter of MKSED is optimized by LSPO, and the optimal length is L=57. From the envelope spectrum, it can be observed that there are obvious peaks in the envelope spectrum at the frequencies of 50 Hz, 100 Hz, 150 Hz, 200 Hz, 250 Hz and 300 Hz, which correspond to the fault frequency and its double, triple, quadruple, quintuple and six times respectively, and the spectrum lines are obvious. The result of the optimization is perfect.

In order to further illustrate the effectiveness of the proposed method for extracting multiple faults, two impulse signals are constructed based on equation 15. The natural frequency of x1 is 300 Hz, and the impulse period is 1/30 s, corresponding to the frequency of 30 Hz. The natural frequency of x2 is 180 Hz, and the impulse period is 1/20 s, corresponding to the frequency of 20 Hz. Figure 16 shows the time domain diagram and envelope spectrum of the simulation signal. It can be observed that the impact is submerged by noise. There is no obvious periodic pulse in the time

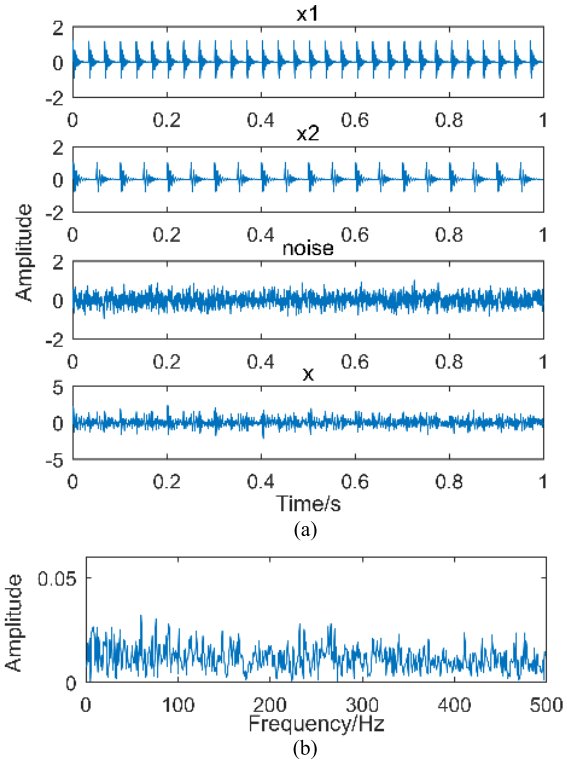

FIGURE 16. Time domain waveform and envelope analysis of simulation signals. (a) Time domain. (b) Envelope spectrum.

domain graph, and the envelope spectrum is also disorderly, which contains a lot of noise.

Figure. 17 is the result of the synthetic signal x decomposition by EEDM. It can be observed that the first layer and the second layer are the components corresponding to signal x_1, and the third layer is the components corresponding to signal x_2. The first layer and the second layer have mode mixing, and then the mode mixing is eliminated by mode reconstruction. The reconstructed results are shown in Figure 18.

Figure. 19 shows the results of the reconstructed components CMF1 and CMF2 processed by MED. Figure 19 (a) shows the results of CMF1. It can be seen from the time domain diagram that the results of MED processing do not show periodic pulses, only individual pulses are obvious, but there is no regularity to follow, and the spectral lines in the envelope spectrum are not obvious. Figure 19 (b) shows the results of CMF2. It can be observed that there are obvious single pulses without periodic impact. Moreover, there is no obvious spectrum of fault frequency (20Hz) in the envelope spectrum. It is obvious that the results obtained by MED are poor and the fault components are not extracted.

Figure. 20 shows the results of the reconstructed components CMF1 and CMF2 processed by MKSED. Figure. 20 (a) shows the results of CMF1. From the time-domain diagram, periodic shocks can be observed in the results of MKSED. Compared with the results of MED, the spectral lines in the envelope spectrum become clearer. Peaks at frequencies

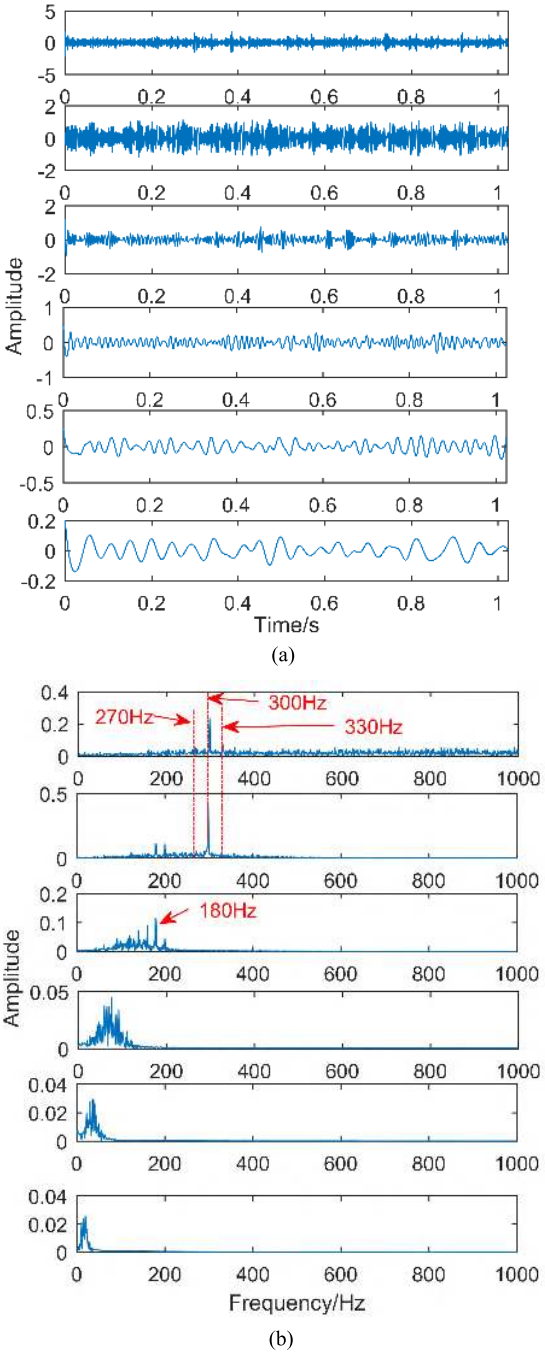

FIGURE 17. The decomposition result of the signal obtained by EEMD. (a) Time domain. (b) Frequency domain.

of 30 Hz, 60 Hz, 90 Hz, 120 Hz and 150 Hz can be observed, which correspond to the fault frequency and its double, triple, quadruple and quintuple respectively. Figure.20 (b) shows the results of CMF 2. It can be observed that there are obvious periodic pulses. Peaks appear at frequencies 20 Hz, 40 Hz, 60 Hz and 80 Hz in the envelope spectrum, the fault frequency and its double, triple, and quadruple respectively. It is obvious that the results obtained by MKSED are obviously better than those obtained by MED. Therefore, the proposed method

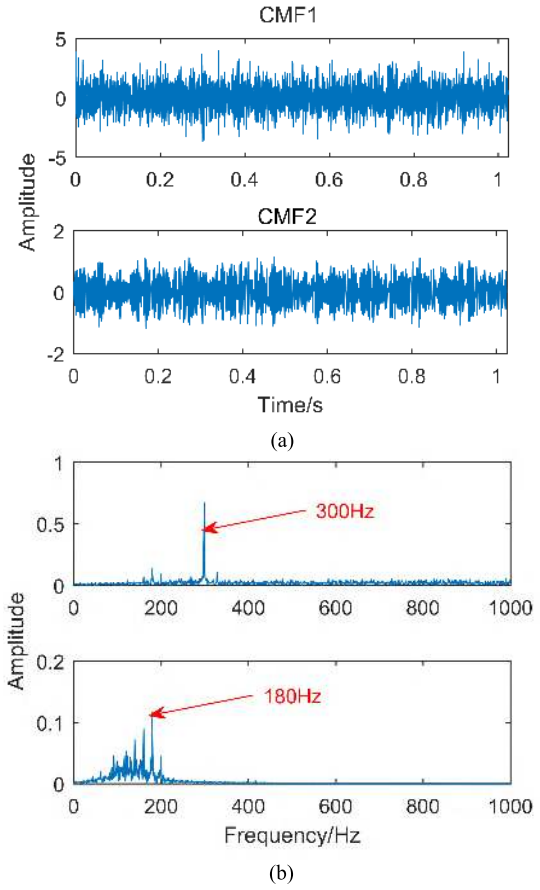

FIGURE 18. The results of mode reconstruction. (a) Time domain. (b) Frequency domain.

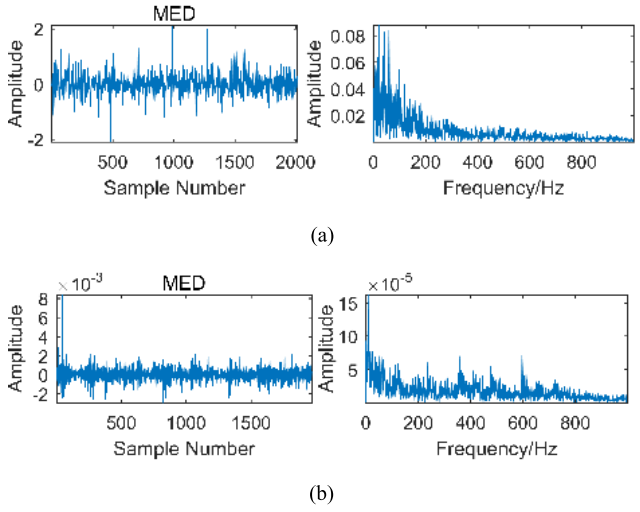

FIGURE 19. The results of the reconstructed components (a) CMF1 and (b) CMF2 processed by MED.

using kurtosis spectral entropy instead of kurtosis as the objective function of deconvolution iteration can improve its performance.

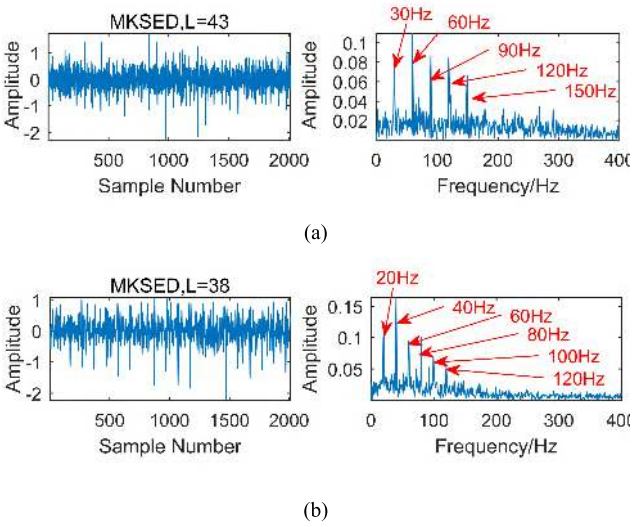

FIGURE 20. The results of the reconstructed components (a) CMF1 and (b) CMF2 processed by MKSED.

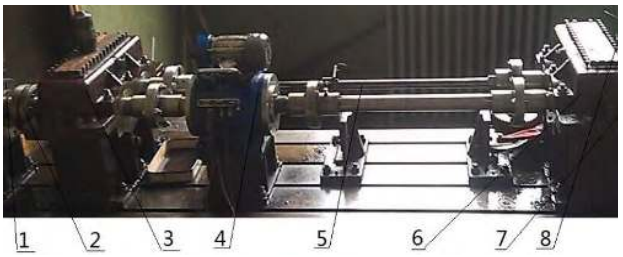

FIGURE 21. The test bench. 1—Speed-adjustable motor, 2—Coupling, 3—Accompanied gearbox, 4—Speed reversing instrument, 5—Torsion bar, 6—Test gearbox, 7—Acceleration sensor 1#, 8—Acceleration sensor 2#.

IV. EXPERIMENTAL VERIFICATION

In order to verify the superiority of the proposed method in engineering application, the closed power flow test bench is used to do relevant experiments. The main components of the test bench include a test gear box, console, motor, a three-way acceleration sensor, etc. The power of the motor is 30KW, and the range of speed adjustment is 120r/min∼1300r/min. The specific experimental platform is shown in Figure. 21. In order to verify the effectiveness of the proposed method, experiments are carried out with flaking defective gears and cracked bearing outer rings. The specific failure form is shown in Figure. 22. The accelerometer for collecting vibration signals is YD77SA. Its sensitivity is 0.01v/ms2, the bearing model is 3222, the sampling frequency is 8000Hz and gear teeth are 18. Through simple calculation, the meshing frequency of gear is 360 Hz and the failure frequency of bearing outer ring is 160 Hz, as shown in Table 1.

Figure. 23 is the time domain diagram and frequency domain diagram of the vibration signal collected by the sensor. From the frequency domain diagram, it can be observed that there are obvious peaks at frequency 360Hz and 720Hz, corresponding to the gear fault frequency and its twice,

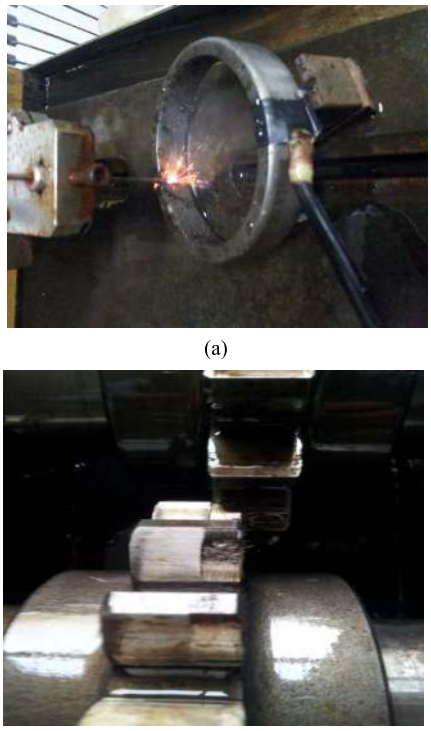

FIGURE 22. Bearing and gear fault diagram. (a) Bearing fault. (b) Gear fault.

TABLE 1. Fault frequency.

Rotation speed	Rotational frequency	Gear meshing frequency	Fault frequency of outer ring
1200rpm	20Hz	360Hz	160Hz

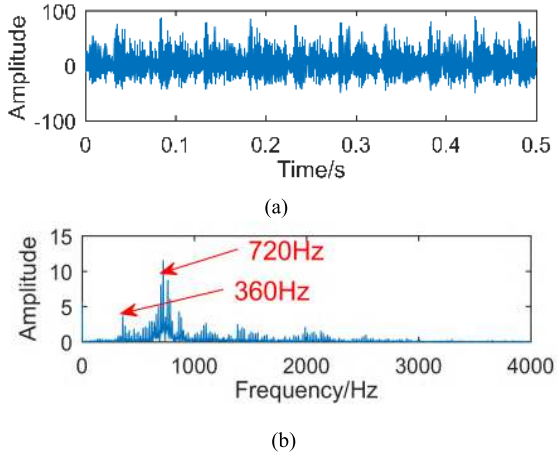

FIGURE 23. Vibration signal. (a) Time domain. (b) Frequency domain.

and the bearing outer ring fault frequency corresponding to 160Hz is submerged by noise.

The fault signal is decomposed by EEMD, and the result is shown in Figure.24. Figure. 24 (a) is a decomposed time

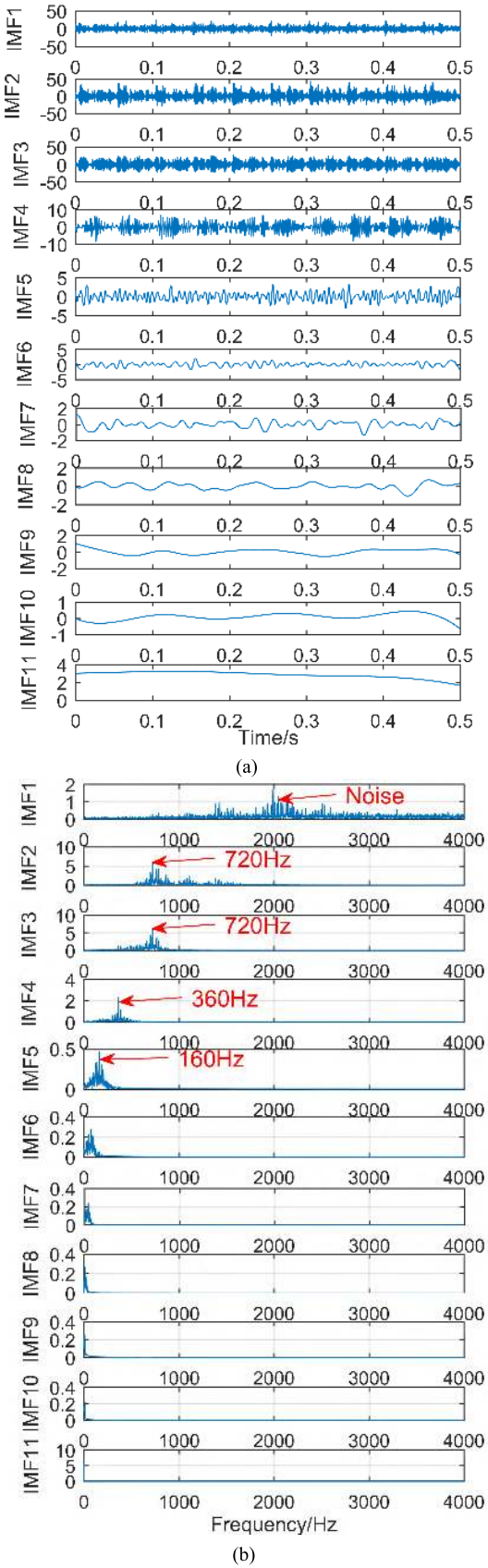

FIGURE 24. The decomposition result of vibration signal obtained by EEMD. (a) Time domain. (b) Frequency domain.

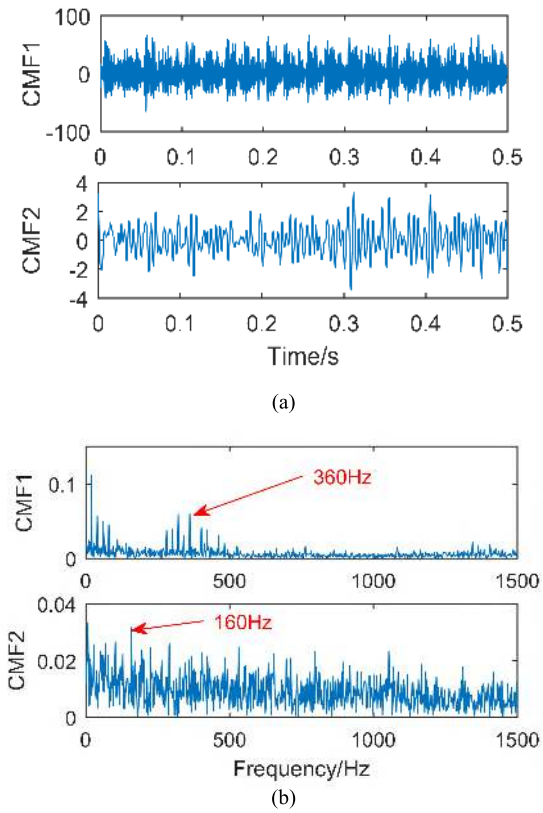

FIGURE 25. The results of mode reconstruction. (a) Time domain. (b) Envelope spectrum.

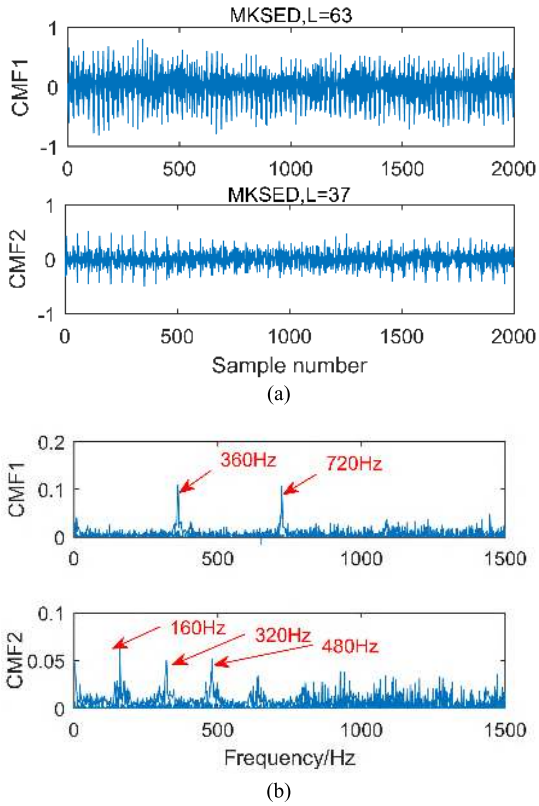

FIGURE 26. The results of the reconstructed components CMF1 and CMF2 processed by MKSED and envelope analysis. (a) Time domain waveform. (b) Envelope spectrum.

domain diagram, and Figure. 24 (b) is a spectrum diagram obtained by spectral transformation. As can be seen from the figure, the signal is adaptively decomposed into 11 layers. The first layer is the high frequency noise component, which does not contain fault information. The second layer has an obvious amplitude at frequency 720, which is twice the gear fault frequency. The third layer is like the second layer. There is an obvious amplitude at the frequency 720, which is twice the gear failure frequency. The fourth layer has an obvious amplitude at frequency 360, which is gear fault frequency. Therefore, the second layer, the third layer and the fourth layer are all fault components of gears. The fifth layer has an obvious amplitude at 160Hz, which is the characteristic frequency of bearing outer ring fault. The layers 6 to 11 do not contain fault information and are pseudo components.

According to the EEMD decomposition results of the vibration signal, firstly, the high-frequency noise component, namely IMF1, is removed. Then the components with mode mixing are reconstructed to eliminate the phenomenon of modal aliasing. That is to say, the components IMF2, IMF3 and IMF4 are reconstructed to CMF1, and IMF5 is CMF2. Finally, the pseudo component, IMF6-IMF11, which does not contain fault information, is removed. The results of mode reconstruction are shown in Figure 25. Figure 25 (b) shows the envelope analysis of the reconstructed component. It can be observed that the fault frequencies of 360 Hz and 160 Hz can be found in the envelope spectrum, but the spectrum lines are cluttered and easy to cause misdiagnosis.

The reconstructed components are processed by MKSED, and the results are shown in Figure 26. It can be observed that the signal is processed by MKSED, and the time domain waveform shows obvious periodicity. Uniform periodic pulses can be clearly observed from time domain illustrations. Figure 26 (b) shows the envelope spectrum of the results of MKSED. It can be observed that there are obvious spectral lines in the envelope spectrum. The extracted frequencies in CMF1 are 360 Hz and 720 Hz, which correspond to gear faults. The frequency extracted in CMF2 is 160Hz and its multiple, which corresponds to the bearing outer ring fault. In order to fully illustrate the advantages of MKSED, the reconstructed signal is processed by MCKD and compared with the results of MCKD.

The reconstructed components are processed by MCKD, and the results are shown in Figure 27. It can be observed that only a limited number of pulses can be extracted by MCKD, which is the result of its principle. Figure 27 (b) shows the envelope analysis of the results of MCKD. Since the number of points (22.22) corresponding to the CMF1 period is not equal to an integer, the MCKD performs the resampling process. This causes the frequency in the envelope spectrum to deviate from the fault frequency. The extracted frequency in CMF2 is 160Hz, but there is only one obvious line. Therefore, the proposed method in this paper is superior to MCKD.

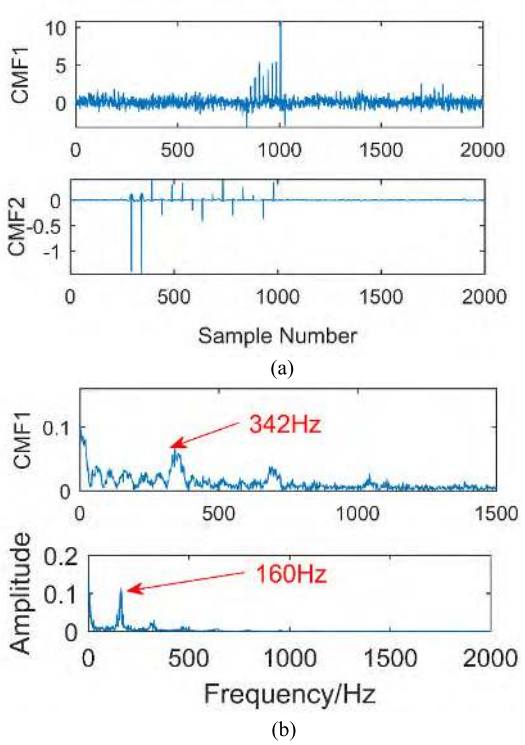

FIGURE 27. The results of the reconstructed components CMF1 and CMF2 processed by MCKD envelope analysis. (a) Time domain waveform. (b) Envelope spectrum.

V. CONCLUSION

Because the minimum entropy deconvolution can only highlight a single impact, it has great limitations in fault diagnosis. Therefore, a maximum kurtosis spectral entropy deconvolution (MKSED) method is proposed and successfully applied to gear box fault diagnosis. The reason why minimum entropy deconvolution can only highlight a single impact is that it takes the maximum peak value as the objective function in the iteration process. In order to highlight the continuous impact, the kurtosis spectral entropy is constructed as an index to measure the effect of the continuous pulse. The maximum kurtosis spectral entropy is taken as the iteration objective, which effectively improves the limitation of MED. Then the kurtosis spectral entropy is used as the objective function of the improved particle swarm optimization algorithm to optimize the MKSED, which effectively overcomes the influence of filter length on the MKSED. Finally, the proposed method is applied to the fault diagnosis of gearbox. The simulation and experimental results prove the effectiveness and superiority of the proposed method.

REFERENCES

[1] Z. Wang, Z. Han, F. Gu, J. X. Gu, and S. Ning, "A novel procedure for diagnosing multiple faults in rotating machinery," *ISA Trans.*, vol. 55, pp. 208–218, Mar. 2015.
[2] W. Du, J. Zhou, Z. Wang, R. Li, and J. Wang, "Application of improved singular spectrum decomposition method for composite fault diagnosis of gear boxes," *Sensors*, vol. 18, no. 11, p. 3804, Nov. 2018.
[3] Y. M. Liu, N. G. Qiao, C. Zhao, and J. J. Zhuang, "Vibration signal prediction of gearbox in high-speed train based on monitoring data," *IEEE Access*, vol. 6, pp. 50709–50719, 2018.
[4] M. Elforjani and E. Bechhoefer, "Analysis of extremely modulated faulty wind turbine data using spectral kurtosis and signal intensity estimator," *Renew. Energy*, vol. 127, pp. 258–268, Nov. 2018.
[5] Y. Xiang, D. Z. Peng, I. R. B. Ubhayaratne, and M. Pereira, "Second-order cyclostationary statistics-based blind source extraction from convolutional mixtures," *IEEE Access*, vol. 5, pp. 2011–2019, 2017.
[6] X. Lang *et al.*, "Fast multivariate empirical mode decomposition," *IEEE Access*, vol. 6, pp. 65521–65538, 2018.
[7] Z. Wei, K. G. Robbersmyr, and H. R. Karimi, "An EEMD aided comparison of time histories and its application in vehicle safet," *IEEE Access*, vol. 5, pp. 519–528, 2017.
[8] F. Jiang, Z. Zhu, and W. Li, "An improved VMD with empirical mode decomposition and its application in incipient fault detection of rolling bearing," *IEEE Access*, vol. 6, pp. 44483–44493, 2018.
[9] Y. Miao, M. Zhao, J. Lin, and Y. Lei, "Application of an improved maximum correlated kurtosis deconvolution method for fault diagnosis of rolling element bearings," *Mech. Syst. Signal Process.*, vol. 92, pp. 173–195, Aug. 2017.
[10] D. He, X. Wang, S. Li, J. Lin, and M. Zhao, "Identification of multiple faults in rotating machinery based on minimum entropy deconvolution combined with spectral kurtosis," *Mech. Syst. Signal Process.*, vol. 81, pp. 235–249, Dec. 2016.
[11] Y. Lei, Z. He, and Y. Zi, "Application of the EEMD method to rotor fault diagnosis of rotating machinery," *Mech. Syst. Signal Process.*, vol. 23, no. 4, pp. 1327–1338, 2009.
[12] M. Z. S. Â¡vokelj and I. Prebil, "EEMD-based multiscale ICA method for slewing bearing fault detection and diagnosis," *J. Sound Vib.*, vol. 370, pp. 394–423, May 2016.
[13] L. Tang, H. Lv, and L. Yu, "An EEMD-based multi-scale fuzzy entropy approach for complexity analysis in clean energy markets," *Appl. Soft Comput.*, vol. 56, pp. 124–133, Jul. 2017.
[14] Z. Wang, Z. Han, and Q. Liu, "Weak fault diagnosis for rolling element bearing based on MED-EEMD," *Trans. Chin. Soc. Agricult. Eng.*, vol. 30, no. 23, pp. 70–78, 2014.
[15] Z. Wang, J. Wang, Y. Kou, J. Zhang, S. H. Ning, and Z. Zhao, "Weak fault diagnosis of wind turbine gearboxes based on MED-LMD," *Entropy*, vol. 19, no. 6, p. 277, Jun. 2017.
[16] H. Endo and R. Randall, "Enhancement of autoregressive model based gear tooth fault detection technique by the use of minimum entropy deconvolution filter," *Mech. Syst. Signal Process.*, vol. 21, no. 2, pp. 906–919, Feb. 2007.
[17] N. Sawalhi, R. B. Randall, and H. Endo, "The enhancement of fault detection and diagnosis in rolling element bearings using minimum entropy deconvolution combined with spectral kurtosis," *Mech. Syst. Signal Process.*, vol. 21, no. 6, pp. 2616–2633, Aug. 2007.
[18] G. L. Mcdonald, Q. Zhao, and M. J. Zuo, "Maximum correlated Kurtosis deconvolution and application on gear tooth chip fault detection," *Mech. Syst. Signal Process.*, vol. 33, pp. 237–255, Nov. 2012.
[19] G. Tang, X. Wang, and Y. He, "Diagnosis of compound faults of rolling bearings through adaptive maximum correlated kurtosis deconvolution," *J. Mech. Sci. Technol.*, vol. 30, no. 1, pp. 43–54, Jan. 2016.
[20] J. Li, M. Li, and J. Zhang, "Rolling bearing fault diagnosis based on time-delayed feedback monostable stochastic resonance and adaptive minimum entropy deconvolution," *J. Sound Vib.*, vol. 401, pp. 139–151, Aug. 2017.
[21] J. Sun, Q. Xiao, J. Wen, and F. Wang, "Natural gas pipeline small leakage feature extraction and recognition based on LMD envelope spectrum entropy and SVM," *Measurement*, vol. 55, pp. 434–443, Sep. 2014.
[22] R. A. Wiggins, "Minimum entropy deconvolution," *Geoexploration*, vol. 16, nos. 1–2, pp. 21–35, Apr. 1978.
[23] S. Kundu, S. Chattopadhyay, I. Sengupta, and R. Kapur, "Multiple fault diagnosis based on multiple fault simulation using particle swarm optimization," *IEEE Trans. Very Large Scale Integr. (VLSI) Syst.*, vol. 22, no. 3, pp. 696–700, 2014.

ZHIJIAN WANG received the Ph.D. degree from the Taiyuan University of Technology, Taiyuan, China. He is currently an Associate Professor with the North University of China. His research interests include mechanical fault diagnosis, signal processing, and intelligent diagnosis. He has published more than a dozen papers in these areas. He is also a member of the Chinese Society of Vibration Engineering.

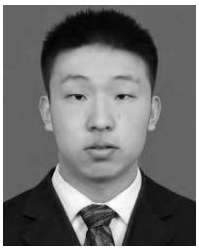

JIE ZHOU received the bachelor's degree from Xi'an Technological University, Xi'an, China, in 2016. He is currently pursuing the master's degree with the School of Mechanical Engineering, North University of China, Shanxi, China. His research interests include mechanical fault diagnosis and signal processing.

JUNYUAN WANG received the Ph.D. degree from the Taiyuan University of Technology, in 2008. He is currently a Professor with the North University of China. His research interest includes intelligent manufacturing technology and systems. He is also the Vice Chairman of the Shanxi Province Society of Vibration Engineering and the Mechanical Transmission Branch of the Shanxi Province Mechanical Engineering Society, and the Executive Director and the Deputy Secretary-General of the Shanxi Province Mechanical Engineering Society.

WENHUA DU received the Ph.D. degree from Tianjin University, Tianjin, China. She was a Visiting Scholar with Warwick University, from 2016 to 2017. She is currently a Professor with the North University of China. Her research interests include mechanical dynamics and machine vision.

JINGTAI WANG received the bachelor's degree in engineering from the College of Information and Business, North University of China, where he is currently pursuing the master's degree. His research interests include mechanical fault diagnosis and signal processing.

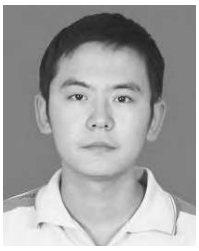

XIAOFENG HAN received the B.S. degree from the North University of China, where he is currently pursuing the master's degree. His research interest includes fault diagnosis of gearbox. He has published a research paper in scholarly journal in the above research area.

GAOFENG HE received the B.S. degree from the College of Information and Business, North University of China, where he is currently pursuing the master's degree. His research interest includes fault diagnosis of gearbox.